Effect of the Environment on Vibrational Infrared and Circular Dichroism Spectra of (S)-Proline

CHIARA CAPPELLI, SUSANNA MONTI, ANTONIO RIZZO

Istituto per i Processi Chimico-Fisici del Consiglio Nazionale delle Ricerche, Area della Ricerca, via G. Moruzzi 1, loc. S. Cataldo, I-56124 Pisa, Italy

Received 1 December 2004; accepted 27 December 2004
Published online 22 March 2005 in Wiley InterScience (www.interscience.wiley.com).
DOI 10.1002/qua.20545

ABSTRACT: The infrared and vibrational circular dichroism of proline in water solution are investigated ab initio employing density functional theory and the integral equation formalism (IEF) version of the polarizable continuum model (PCM). Three solvent models are exploited to evaluate solvent effects in the 1000–2000 cm^{-1} frequency range: a pure implicit continuum approach, a pure explicit model (limited to three solvent molecules), and a combined specific/continuum approach. Effects on spectra arising from different protonation states (neutral, zwitterionic, cationic, and anionic) are analyzed. Int J Quantum Chem 104: 744–757, 2005

Key words: PCM; solvent effects; DFT; VCD; proline

1. Introduction

The importance of proline—one of the 20 natural amino acids, and a very special one among the set owing to some peculiar structural features and properties—has been properly emphasized in the literature in several instances. Proline is a basic constituent of proteinic and peptide structures [1–9]. Its pyrrolidine ring, with an imino group attached to it, is unique among natural amino acids. Its ring is less flexible than in most other amino acids. Proline is one of the most abundant amino acids forming collagen polypeptide chains, which are almost repeating units of a tripeptide segment Gly-X-Pro where X is another amino acid residue. Its ring puckering, together with the trans/cis ratio of the X-Pro peptide bonds, are important factors influencing the stability of this very abundant protein.

Early studies of polyphenol/protein binding suggested that polyphenols bind preferentially to proline residues [10]. More recent articles have shown that the interaction is primarily a hydrophobic association between these amino acids and aromatic phenolic rings [11, 12]. These and other properties make proline a most interesting and widely studied reference system.

The structure of proline has been the subject of several experimental and computational studies. X-ray crystallography [13–15], electron diffraction [16, 17], microwave [18–25], nuclear magnetic reso-

Correspondence to: A. Rizzo; e-mail: rizzo@ipcf.cnr.it
C. Cappelli is currently affiliated with Polylab–INFM, Pisa.

nance [26], low-resolution photoelectron spectroscopy [27, 28], and infrared (IR) [29–31] techniques have been employed. Solid proline has been shown to assume a zwitterionic form [13], absent in polypeptide chains [13]. On the other hand, it is well known that proline in the gas phase assumes a neutral non-zwitterionic structure. Most recently matrix isolation IR spectroscopy [29, 31] has been instrumental in yielding precious structural information. Reference [31] is of special relevance for the present study, because it includes both an experimental and an ab initio analysis of the IR spectra of proline. Other computational ab initio studies include Refs. [32–35] and the rather recent Ref. [36]. Benzi and co-workers [37] studied the conformational behavior of some dipeptide derivatives of proline and hydroxyproline both as isolated molecules and in aqueous solutions.

Our scope in this article is to analyze the IR and vibrational circular dichroism (VCD) spectra of proline in the gas phase and in water. We are thus interested both in the structural and conformational properties of the amino acid and in its response to IR radiation. Response properties of proline were the subject of some recent studies done by one of the present authors. Both natural optical activity (NOA) [38] and magnetochiral birefringence (MB) [39] of proline in the gas phase were investigated in some detail. These studies involved a determination and a detailed study of several conformers of proline, in the neutral form and for both the protonated and deprotonated species, made employing density functional theory (DFT) with the Becke three-parameter Lee–Yang–Parr (B3LYP) functional [40–42]. The subsequent analysis of the linear (NOA) [38] and nonlinear (MB) [39] response to electromagnetic radiation (in the latter case in the presence of a static magnetic induction field parallel or antiparallel to the direction of propagation of light) was performed employing analytic response theory at the DFT [38] or Hartree–Fock [38] levels of theory. The conformational investigation made in Refs. [38] and [39] yielded the starting guess for the geometries of the structures of proline studied here.

We extend now our interest to infrared properties, in particular to IR and VCD spectra [43], by performing an ab initio study of the effect of environment, i.e., solvent, to the spectra. Both IR and VCD are widely employed techniques, of paramount importance in the analysis of molecular vibrations. VCD spectroscopy [43] in particular is a well established technique for organic conformational analysis, and it allows for an efficient determination of the absolute configuration of chiral compounds.

In this article, solvent effects are treated by using the integral equation formalism (IEF) [44–46] version of the polarizable continuum model (PCM) [47–50]. The solvent is modeled as a continuum, infinite, homogeneous, and usually isotropic dielectric medium, and its response to the presence of the solute depends on the dielectric constant ϵ. The solute is hosted into a molecularly shaped cavity, and the evaluation of the mutual interaction between solute and solvent is achieved by introducing an apparent charge distribution spread on the cavity surface.

The extension of IEF to the evaluation of IR and VCD spectra was presented in Refs. [51] and [52].

2. Computational Details

All the calculations were performed using DFT with the B3LYP hybrid functional [40–42] and the 6-31+G(d) basis set. The reliability of DFT for IR and VCD calculations has been widely assessed, (see, e.g., Refs. [53, 54]). The Gaussian program [55] was used for the calculations both for the isolated systems and in solution. The determination of infrared and VCD spectra in solution was performed using analytical derivative methods in the equilibrium framework [56] within the double harmonic approximation. Gauge-including atomic orbitals (GIAOs) [57–59] have been exploited in all cases for the calculation of VCD spectra [60].

The results in water solution were obtained by assuming values of $\epsilon_0 = 78.39$ and $\epsilon_{inf} = 1.776$ for the static and the optical permittivities, respectively. The geometries of all the systems have been optimized in the appropriate phase. The cavity used was of molecular shape and built by interlocking spheres with the following radii: 2.4 Å for carbon, CH, and CH_2 groups, 2.04 Å for nitrogen, 1.44 Å for hydrogen, and 1.824 Å for oxygen. Only the electrostatic component of the solute–solvent interaction was taken into account in the IR and VCD calculations, whereas non-electrostatic repulsion, dispersion, and cavity contributions have been included for the calculations of free energies and Boltzmann factors [49]. All the calculations of VCD spectra were carried out on the (S) conformation of proline.

3. Results and Discussion

3.1. CONFORMATIONAL ANALYSIS

For a discussion of the conformers of neutral (zwitterionic and non-zwitterionic), cationic and

TABLE I

Conformations of neutral non-zwitterionic proline, as isolated molecule (vac) and with the IEF continuum (solvent is water, IEF) and again without dielectric continuum and with the explicit inclusion of three water molecules (3W).

System	Phase	τ1	τ2	τ3	τ4	d(OH . . . N)	∠(OH . . . N)	d(CO . . . HN)	∠(CO . . . HN)
N1	vac	179.8	179.0	127.9	21.7	1.87	127.9		
N2	vac	−178.5	177.5	124.3	−24.5	1.90	127.2		
N3	vac	−0.38	−6.20	−135.6	−13.8			2.36	106.0
N4	vac	−0.75	−18.9	−105.7	10.2			2.26	111.5
N1	IEF	179.6	178.2	128.1	20.8	1.79	129.7		
N2	IEF	−178.6	178.1	123.1	−23.9	1.81	129.1		
N3	IEF	−0.75	−8.11	−135.1	−14.3			2.39	105.9
N4	IEF	−1.52	−21.4	−93.3	−0.67			2.32	107.8
N1 + 3W	vac	−179.5	176.9	128.0	20.6	1.78	129.8		
N2 + 3W	vac	−178.4	176.7	125.2	−25.5	1.81	128.7		
N1 + 3W	IEF	−179.0	176.9	129.5	19.9	1.78	130.8		
N2 + 3W	IEF	−178.8	178.6	123.6	−24.1	1.74	130.2		

The torsional parameters are the cis or trans orientation of the OH and CO groups (τ1), the orientation of the carboxylic group (τ2) and of the NH (τ3) bond with respect to the ring; and the ring puckering (τ4) (see Fig. 1).
Also shown are the OH . . . N and CO . . . NH distances, in Å, and the corresponding angles.

anionic structures of (S)-proline we refer to Tables I and II, reporting the relevant structural parameters (see Fig. 1); to Table III, displaying the results we obtain for the free energies (G_{corr}), the dipole moments (μ) and Boltzmann factors (Bf); and to Figures 2 and 3, showing the 3-D arrangement of the different conformers studied in this work.

Conformational isomers of neutral, anionic, and cationic proline have been investigated previously by means of various experimental techniques and high-level ab initio calculations, (see [38] and references therein). Therefore we selected, as starting points for our studies, the four conformers of lowest energy taken from Ref. [38]. According to the

TABLE II

Cationic (C), anionic (A), and zwitterionic (Z) proline conformations as isolated system and with the IEF continuum (solvent is water).

System	Phase	τ1	τ2	τ3	τ4	d(CO . . . HN)	∠(CO . . . HN)
C1	vac	0.38	−3.88	125.26/−118.4	23.0	1.95/3.27	119.4/43.2
C2	vac	0.15	−5.42	125.4/−118.3	26.2	2.00/3.28	116.9/44.0
C3	vac	179.1	−5.15	124.0/−119.6	−24.6	1.94/3.26	118.6/42.8
C1	IEF	−0.52	−5.14	125.2/−118.4	22.5	2.07/3.33	115.5/43.4
C2	IEF	−0.26	−6.00	126.0/−117.7	−27.3	2.13/3.33	112.8/45.0
C3	IEF	177.8	−8.81	127.7/−116.0	−28.5	2.11/3.31	113.4/45.0
A1	vac		171.6/−9.38	−120.3	−22.3	2.07	118.3
A2	vac		−135.2/47.03	173.4	−29.6	2.55	94.6
A3	vac		122.6/−59.21	84.4	−10.6	3.93	13.9
A1	IEF		163.3/−17.8	−108.3	−30.6	2.17	114.6
A2	IEF		38.8/−143.1	167.1	−27.9	2.65	88.8
A3	IEF		131.1/−50.5	103.6	−11.9	3.86	21.1
Z1	IEF		178.0/−1.81	123.6/−120.7	25.0	1.85/3.23	123.9/42.8
Z2	IEF		175.0/−5.92	126.1/−118.2	−25.8	1.91/3.24	120.8/44.2
Z1 + 3W	IEF		175.0/−5.32	125.7/−118.4	23.0	1.90/3.25	121.0/43.2
Z2 + 3W	IEF		174.5/−6.50	125.0/−118.9	−25.5	1.97/3.27	117.9/43.5

See Table I for details.

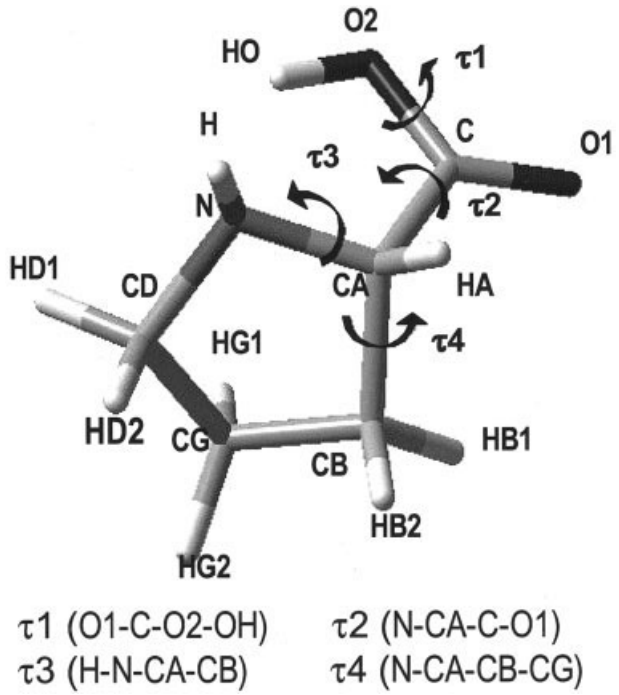

FIGURE 1. The torsional angles employed in the discussion of the conformers of proline.

relative energies given there [38], selecting these conformers accounts for more than 98% of the Boltzmann population in the gas phase. The set of initial structures was fully reoptimized both in the gas phase and in water solution at the DFT-B3LYP/6-31+G(d) level, and the stationary points found were characterized by harmonic frequencies calculations. Differences in bond lengths and bond angles among the various conformers were found to be rather small. Therefore only four torsion parameters are reported in Table I and II. They describe both in the gas phase and in solution the cis or trans orientation of the OH and CO groups (τ1), the orientation of the carboxylic group (τ2) and of the NH (τ3) bond with respect to the ring, and the ring puckering (τ4). A scheme intended to show how these torsional parameters are defined is given in Figure 1.

3.1.1. Neutral Non-zwitterionic Proline Structures

The four neutral non-zwitterionic conformers of proline discussed in this work are labelled **N1, N2,**

TABLE III

Calculated B3LYP/6-31+G(d) free energies (G_{corr}) with thermal and zero-point corrections included and normalized Boltzmann factors (Bf) for the various conformations of proline as isolated molecule, at 298 K and 435 K, and in water solution at 298 K.

	Isolated				In water			
System	G_{corr}	Bf (298 K)	Bf (435 K)	μ/D	G_{corr}	G_{nel}/(kcal · mol^{-1})	Bf (298 K)	μ/D
N1	−401.060786	0.47256[a]	0.41402	5.9951	−401.077150	1.82	0.54144	7.8545
N2	−401.060568	0.37513	0.35337	6.1100	−401.076928	1.78	0.45789	7.9377
N3	−401.059387	0.10739	0.15002	1.7976	−401.070643	2.08	0.00035	2.4703
N4	−401.058564	0.04492	0.08259	2.1464	−401.070469	2.05	0.00031	3.0369
N1 + 3W	−630.306528	0.84700		8.0898	−630.336449	7.40	0.78666	9.8896
N2 + 3W	−630.304914	0.15300		8.3120	−630.334946	7.23	0.21334	13.6886
C1	−401.414846	0.52143[b]			−401.506663	2.03	0.27594	
C2	−401.414765	0.47857			−401.507538	2.01	0.72101	
C3	−401.401361	n			−401.502376	2.01	0.00305	
A1	−400.526413	0.99922[c]			−400.626561	1.98	0.92389	
A2	−400.519653	0.00078			−400.624162	1.97	0.07405	
A3	−400.514791	n			−400.621260	2.27	0.00206	
Z1	unstable				−401.082508	1.96	0.49234	13.9145
Z2	unstable				−401.082521	1.95	0.50766	14.3362
Z1 + 3W					−630.348383	7.13	0.14241	16.8153
Z2 + 3W					−630.349887	7.01	0.85759	20.0246

Dipole moments (μ) for the neutral species and nonelectrostatic contributions (G_{nel}) are also included. "n" indicates a negligible Bf. Atomic units, unless specified otherwise.

[a] Cf. **N1:** 0.553; **N2:** 0.292; **N3:** 0.078; **N4:** 0.077, from data in Ref. [38]. **N1:** 0.570; **N2:** 0.254; **N3:** 0.118; **N4:** 0.055, from results labelled "CCSD(T)-6-31++G**//MP2/aug-cc-pVDZ", Ref. [31].

[b] Cf. **C1:** 0.584; **C2:** 0.416; **C3:** 0.000, from data in Ref. [38].

[c] Cf. **A1:** 0.999; **A2:** 0.001; **A3:** 0.000, from data in Ref. [38].

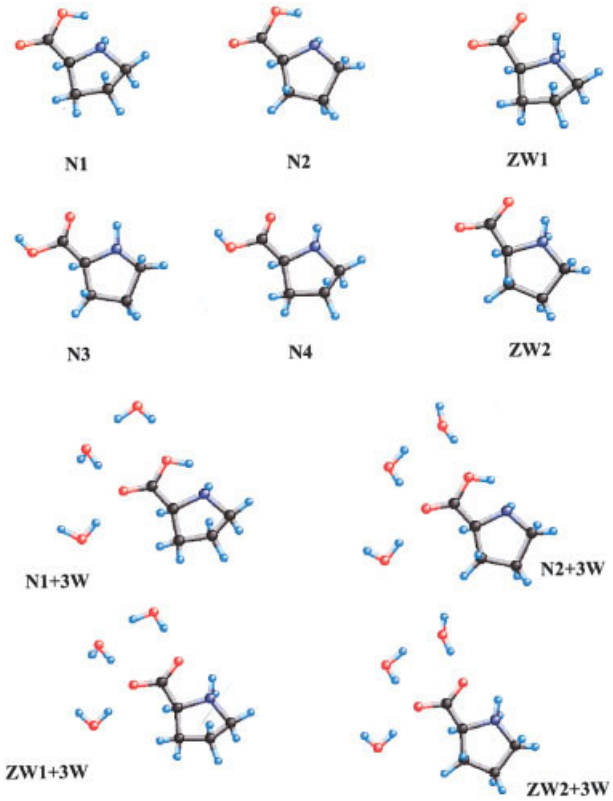

FIGURE 2. The neutral optimized (including zwitterionic) structures of isolated proline and of proline clusters with three water molecules explicitly included. [Color figure can be viewed in the online issue, which is available at www.interscience.wiley.com.]

N3, and **N4,** (Fig. 2). The first two minimum energy structures, **N1** and **N2,** correspond to conformations where the OH group arranges to form practically planar five-membered rings. This arrangement yields intramolecular O—H . . . N hydrogen bonds with O—H . . . N distances of 1.87 Å and ∠O—H . . . N angles of about 128°.

The ring puckering ($\tau 4$) is different in the four structures. The **N1** and **N4** conformers have an exo form whereas for the **N2** and **N3** geometries an endo form is observed. The OH and CO groups are trans to each other in the **N1** and **N2** geometries whereas they take a cis relative position in the **N3** and **N4** conformers as shown by the values of $\tau 1$ reported in Table I. Torsion angles $\tau 1$, $\tau 2$, and $\tau 3$ of **N1** and **N2** are similar, whereas the deviations between **N3** and **N4** exceed 12° in the worst case ($\tau 3$). The orientation of the CO group in **N3** and **N4** allows the formation of an N—H . . . O═C intramolecular hydrogen bond with distances of about 2.3 Å. This bond forms only part of a five-membered ring that is never close to being planar. As a matter of fact the strong hydrogen bond interaction observed in structures **N1** and **N2** is principally responsible for the increased stability of these proline conformers.

Optimization in solution does not change substantially the torsion parameter discussed above, the only remarkable exception being structure **N4** where $\tau 3$ and $\tau 4$ are about 10° smaller than the corresponding values in the gas phase. There are, however, notable differences in the hydrogen bond lengths and angles. Passing from the isolated molecule to solution a shortening of the N . . . H—O distance and an increase of the donor-H-acceptor angle ∠O—H . . . N is observed.

Although we have used the DFT method with a medium-quality basis set, the reliability of our analysis is confirmed by the satisfactory agreement of the relative energy results presented in Table III with those obtained with higher quality calculations [31, 36, 38]. The data in Table III clearly confirm the coexistence, at normal temperatures, of at least two conformers of neutral non-zwitterionic proline.

The energy ordering of the four structures is maintained in solution, but population-wise conformers **N3** and **N4** practically disappear, leaving only conformers **N1** and **N2** with a population ratio almost equal to that found in the gas phase. Solvation energies are larger for molecular structures with larger dipole moments, as expected.

Our aim is to evaluate the effect of the aqueous environment on the IR and VCD spectra of neutral proline. The very peculiar behavior of water as solvent, yielding specific solute–solvent interactions, coupled to the "local" character of vibrational mo-

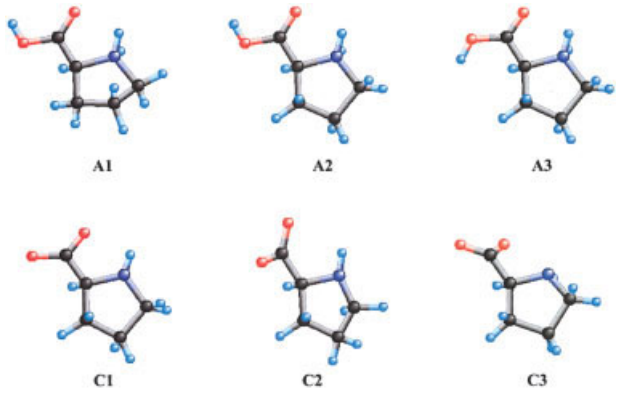

FIGURE 3. The charged optimized (anionic, **A1** to **A3;** cationic, **C1** to **C3**) structures of isolated proline. [Color figure can be viewed in the online issue, which is available at www.interscience.wiley.com.]

tions, calls for more suitable approximations. Thus, structures including explicit water molecules around the neutral structure (both non-zwitterionic and zwitterionic, see also below) were designed and introduced in our study. In some instances in the following these clusters will be collectively labelled **N + 3W** and **Z + 3W,** for non-zwitterions and zwitterions, respectively. In particular, three water molecules were added to the most populated non-zwitterionic conformers **N1** and **N2** (yielding the forms labelled **N1 + 3W** and **N2 + 3W,** see Fig. 2) and the resulting structures were optimized. The solvent molecules are oriented in such a way that the hydrogens of two of them point toward the carbonyl oxygen of the COOH group, thus forming intermolecular hydrogen bonds with distances of 1.95 and 1.90 Å for **N1 + 3W** and 1.94 and 2.14 Å for **N2 + 3W,** respectively. The ∠donor—H . . . acceptor angles are 156.0° and 174.3° for **N1 + 3W** and 155.7° and 162.5° for **N2 + 3W,** respectively. The third water molecule is located near the hydroxylic oxygen at an O . . . H(water) distance of 2.28 Å and a ∠donor—H . . . acceptor angle of 158.1° for **N1 + 3W.** The corresponding values for **N2 + 3W** are 1.99 Å and 168.0°, respectively. As far as the geometry of the **N1** and **N2** moieties is concerned, only small deviations from the conformations of the isolated systems are observed.

By including the IEF continuum on these **N + 3W** clusters, the geometry of the proline moiety is not substantially affected, whereas the position of the water molecules changes so that the resulting (carbonyl)O—H(water) distances become 1.87 and 1.90 Å for **N1 + 3W** (IEF) and 1.90 and 1.96 Å for **N2 + 3W** (IEF). The (hydroxyl)O—H(water) distances are 2.15 Å and 1.98 Å for **N1 + 3W** (IEF) and **N2 + 3W** (IEF), respectively. The carbonyl ∠donor—H . . . acceptor angles change to 172.8° and 179.9° for **N1 + 3W** (IEF) and 171.4° and 176.0° for **N2 + 3W** (IEF). The hydroxy ∠donor—H . . . acceptor angles become 155.6° for **N1 + 3W** (IEF) and 163.7° for **N2 + 3W** (IEF).

As far as the Boltzmann population of the **N + 3W** clusters are concerned, the **N1** original conformer is predominant. The weights are ≈0.847 for **N1 + 3W** and ≈0.153 for **N2 + 3W.** A slight variation is observed following the inclusion of the IEF continuum [≈0.787 for **N1 + 3W** (IEF) and ≈0.213 for **N2 + 3W** (IEF), with the inclusion of nonelectrostatic terms to the solvation free energy at 298K, see Table III].

3.1.2. Cationic Proline Structures

Because of the protonation of the nitrogen atom in the cationic structures, only a hydrogen bond of type N—H . . . O═C can be present in the whole set of conformers (see Fig. 3). The difference between the lowest energy conformer **C1** and second most stable structure **C2** is in the ring puckering (Table II and Fig. 3). The third conformer, labelled **C3,** displays values of $\tau 2$, $\tau 3$, and $\tau 4$, similar to those seen for **C2,** but it differs in the COOH arrangement, with the OH and CO groups assuming a trans relative position. Optimization in solution causes a general increase of the O . . . H—N distances, whereas major variations in torsion angles are observed for structure **C3.**

As in the case of neutral non-zwitterionic proline the relative energies of cationic proline conformers are in agreement with the values found in Ref. [38]. The order of stability is, however, interchanged in solution and the **C2** structure is predicted to be more stable than the most stable conformer in the gas phase (**C1**) by ≈0.5 kcal · mol^{-1}.

3.1.3. Anionic Proline Structures

The three most stable anionic structures of proline examined here are quite different from each other (see Fig. 3). The lowest energy (**A1**) and the second minimum energy (**A2**) conformers, both displaying an endo puckering, differ in both the arrangement of the COO^- group and the orientation of the NH bond with respect to the ring. In **A1** the NH hydrogen is arranged upward, toward the carboxylic group, thus favoring the formation of an intramolecular hydrogen bond with a N—H . . . O═C distance of 2.07 Å and a ∠donor—H . . . acceptor angle of about 118°. This is the highest value found for the set of anionic conformers. On the contrary, in **A2** the NH hydrogen points downwards opposite to the carboxylic oxygens and a larger N—H . . . O═C distance (2.55 Å) and a narrower ∠donor—H . . . acceptor angle (≈95°) are observed. The intramolecular hydrogen bond interaction is reduced in conformer **A2** and almost absent in **A3,** where the shortest N—H . . . O═C distance is ≈3.9 Å and the ∠NH . . . O angle is ≈14°. **A3** is the structure of highest energy and it has an exo puckering of the pyrrolidine ring.

When the minimum energy conformations obtained in the gas phase are reoptimized in solution, the torsion angles change very little for the **A1** and **A2** structures, with a maximum difference of about 12°. A substantial rearrangement is observed instead for structure **A3,** where the largest deviation of dihedral angles is of about 23° and the ring puckering changes from exo to endo.

The relative energies of the anionic proline conformers agree with those reported in Ref. [38]. The

energy ordering of the three structures is also maintained in solution.

3.1.4. Zwitterionic Proline Structures

Our calculations in the gas phase do not yield stable zwitterionic forms of proline, as observed also in Ref. [38]. Zwitterionic forms are highly unstable, and the non-zwitterionic character of proline in the gas phase has also been demonstrated by the analysis of experimental data in Ref. [31]. Two stable conformers, differing in the ring puckering, are found instead in aqueous solution.

The structure of a molecule in water is due to the delicate balance of intramolecular and intermolecular interactions between the molecule and the surrounding solvent. It is well known that the non-zwitterionic form in amino acids is energetically favored in the gas phase, whereas amino acids in water exist as zwitterions over a large pH range [13, 38]. Our calculations confirm the tendency of water to preferentially stabilize the zwitterionic form of proline. In fact, the zwitterion is about 3.4 kcal · mol^{-1} lower in energy than the non-zwitterionic form at the B3LYP/6-31+G(d) level of theory.

Similarly to neutral structures, the effect of explicit solute–solvent interactions is here evaluated by adding three water molecules near the carboxylic group and then surrounding the clusters with the polarizable continuum, thus yielding the cluster structures labelled collectively (**Z + 3W** (IEF)). The orientation of the water molecules is very similar to that seen for the **N1 + 3W** and **N2 + 3W** conformers: the hydrogens of two of the solvent molecules point toward one carboxylic oxygen forming two intermolecular hydrogen bonds with distances of 1.81 and 1.78 Å for **Z1 + 3W** (IEF) and 1.81 and 1.86 Å for **Z2 + 3W** (IEF) respectively. The ∠donor—H . . . acceptor angles were 176.7° and 175.8° for **Z1 + 3W** (IEF) and 176.2° and 172.5° for **Z2 + 3W** (IEF), respectively. The third water molecule is hydrogen bonded to the other carboxylic oxygen at an O . . . H(water) distance of 1.87 Å for **Z1 + 3W** (IEF) and 1.78 Å for **Z2 + 3W** (IEF), whereas the ∠donor—H . . . acceptor angles are 171.6° for **Z1 + 3W** and 175.4° for **Z2 + 3W** (IEF). The torsion angles (τ2), (τ3), and (τ4) are similar to those obtained for the same structures after optimization in solution with the continuum approach, with a maximum difference of ≈3°. Instead, a remarkable lengthening of the CO . . . NH distances is observed.

As noted before, theoretical calculations indicate that the addition of three water molecules and of the continuum solvation model to the non-zwitterionic form of proline yield a local minimum on the potential energy surface. However, the zwitterionic form remains still noticeably lower in energy than the non-zwitterionic by more than 8 kcal · mol^{-1}. Changes in the hydroxyl bond length are observed when the most stable conformations of neutral proline (**N1** and **N2**) are surrounded by solvent treated with models of increasing complexity.

Indeed, going from the gas phase to the solution a general increase of the OH bond length (between 0.01 and 0.04 Å) with a simultaneous decrease of the OH . . . N distance are observed. The largest variation is found for the **N + 3W** clusters when the IEF continuum is included. This is indeed consistent with the stabilization of the zwitterionic form found in water: in fact, as the OH distance increases, the neutral structure tends toward the zwitterion.

3.2. PREDICTION OF IR AND VCD SPECTRA

All the spectra reported in this work were simulated using Lorentzian-shaped bands with 10 cm^{-1} full width at half maximum. Only the range between 1000 and 2000 cm^{-1} is displayed and discussed, as it is well known that anharmonic contributions dominate the spectrum below 1000 cm^{-1}, and our calculations are limited to a purely harmonic approach. In addition, the basis set we are using, 6-31+G(d), yields only a rough description of the electronic density at the hydrogen atoms. For this reason the part of the spectrum between 3000 and 4000 cm^{-1}, dominated by the OH and CH stretching modes, is likely to be poorly reproduced by our approach. We further note that the analysis reported in the following paragraphs is focused on the effects of the water solvent on proline vibrational spectra. Given the vibrational frequency of the water OH stretching modes falls within the 3000–3500 cm^{-1} range, the spectra of proline dissolved in water are dominated in that range by these contributions and our analysis would be meaningless.

3.2.1. The Isolated Molecule in the Neutral Non-zwitterionic Form

IR spectra of the individual **N1–N4** conformers of neutral proline in the gas phase are shown in Figure 4. Their appearance is widely different going from a conformer to the other. In particular, large differences are observed between the spectra of the internally H-bonded conformers (**N1** and **N2**) and

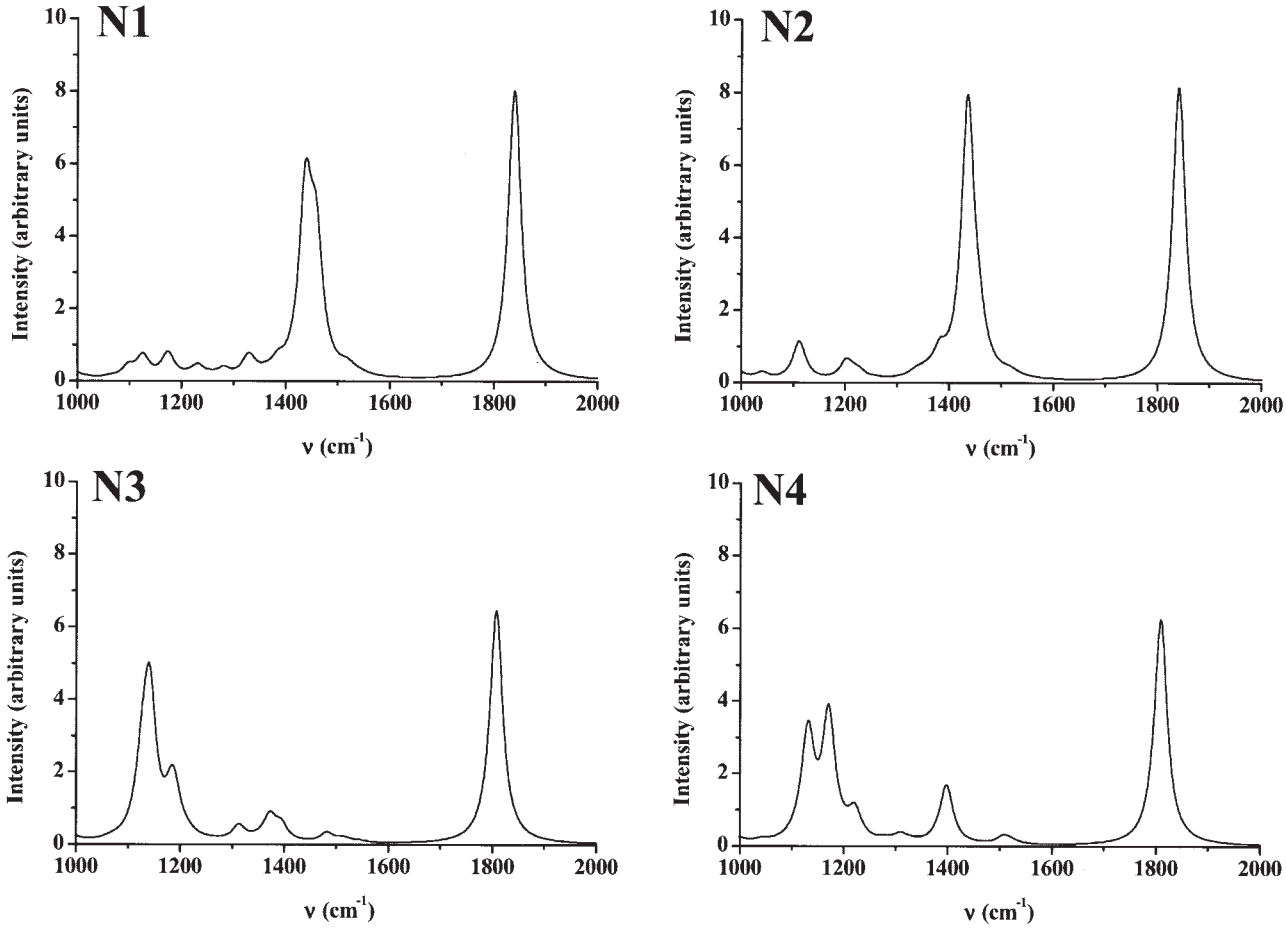

FIGURE 4. IR spectra of the individual neutral non-zwitterionic proline conformers in the gas phase, in the 1000–2000 cm^{-1} frequency range.

the non-H-bonded conformers (**N3** and **N4**). Indeed, as expected, the peak around 1800 cm^{-1} (due to the carbonyl stretch) is shifted to higher frequencies (by about 30 cm^{-1}) by H-bond effects, whereas its intensity is almost unaffected by H-bond interactions. More sensitive to internal H-bond are bending vibrations, which span the region between 1100 and 1560 cm^{-1}. The analysis of the calculated normal modes for these bands shows that this portion of the spectrum is associated to normal vibrations of the whole molecules, resulting from a complex merging of the (carbonyl)C—O—H bending with the (ring)C—N—H bend and with ring and CH_2 bending vibrations. Indeed, the number and position of bending bands are almost the same for all the four conformers, but the individual intensity of each band, and even the intensity ratios, largely change passing from the internally H-bonded complexes to the non-H-bonded. Such changes in intensities result in totally different spectra, so that in the case of **N1** and **N2** the spectrum in this region is dominated by the complex and strong band centered around 1450 cm^{-1}, whereas for **N3** and **N4** the dominant absorption is due to the broad and structured band between 1100 and 1200 cm^{-1}.

The experimental IR spectrum of matrix isolated proline was reported in Ref. [31]. Besides the modes located in the region covering the 3000–3600 cm^{-1} range, modes which, see above, we are not able to reproduce reasonably, a vibrational mode of proline that is sensitive to differences in H-bonding is the stretching vibration of the carbonyl group (in the 1700–1900 cm^{-1} region). A double peak, attributed to the presence of two conformers of proline (with and without internal H-bond) in approximately equal amounts was found experimentally in this region [31].

To assess the quality of the computational approach exploited in this study and to be able to compare calculated and experimental spectra, an ab

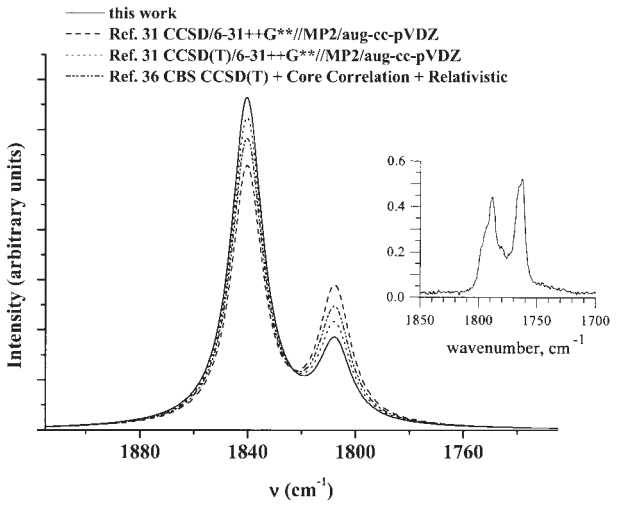

FIGURE 5. The calculated IR spectrum of neutral non-zwitterionic proline in the gas phase in the 1725–1925 cm^{-1} region (solid curve). The experimental spectrum [31] is in the inset. Also shown are the simulated spectra obtained by using our B3LYP/6-31+G(d) frequencies and intensities together with Boltzmann populations taken from the literature [31, 36, 38]. The temperature is 435 K.

initio "statistically averaged" spectrum was obtained from appropriately weighted spectra of the individual conformers. The Bf, calculated for the various conformations of neutral non-zwitterionic proline, are reported in Table III. Both zero-point energy (ZPE) and thermal corrections (at 298 K and 435 K, not scaled) were taken into account when obtaining Boltzmann populations.

The calculated IR spectrum of neutral proline in the gas phase in the 1725–1925 cm^{-1} region is reported in Figure 5. As a further comparison, the experimental spectrum and simulated spectra obtained by using our B3LYP/6-31+G(d) frequencies and intensities together with Boltzmann populations taken from the literature [31, 36, 38] are also included in the figure. All the calculated values refer to 435 K, the experimental temperature. Our B3LYP/6-31+G(d) ZPE and thermal corrections were included in the calculation of populations at 435 K from the values taken from the literature [31, 36, 38].

Figure 5 shows that none of the approaches actually succeeds in reproducing correctly the experimental intensity pattern, although the intensity of the band at lower frequency is a bit increased as the quality of the quantum mechanical level increases. For this reason, the analysis in the following sections is limited to DFT.

3.2.2. Neutral Non-zwitterionic Proline in Water: IR and VCD Spectra

To determine the effects of solvent on the vibrational spectra of proline, three different methodologies were applied. The first is a pure implicit solvation model, namely the continuum IEF approach, which should be able to account for dielectric effects. Because of the nature of the solute (proline) and solvent (water), it is reasonable to expect that specific solute–solvent hydrogen bonding effects might play a relevant role in the prediction of vibrational spectra. These specific effects are here somehow accounted for by using an explicit-only solvation model, based on the clusters discussed previously (Fig. 2, **N + 3W**). As a further refinement, a third model is also used, obtained by surrounding the clusters with the IEF continuum.

As pointed out above, the relative weight of the four neutral proline conformations changes as a result of the inclusion of the IEF continuum. In particular, as expected, solvent effects favor the structures with intramolecular hydrogen bonding (**N1** and **N2**) over the others. As a result, the Boltzmann weight of the noninternally bonded molecules becomes negligible in the condensed phase. Such behavior is reflected in the predicted spectra. The averaged spectra of neutral proline in the gas phase and in aqueous environment are reported in Figure 6. The calculated spectra were obtained by averaging over the four conformations on the basis of their Boltzmann weights. The inclusion of the IEF continuum not only shifts the predicted bands to lower frequencies (as expected), but it also induces

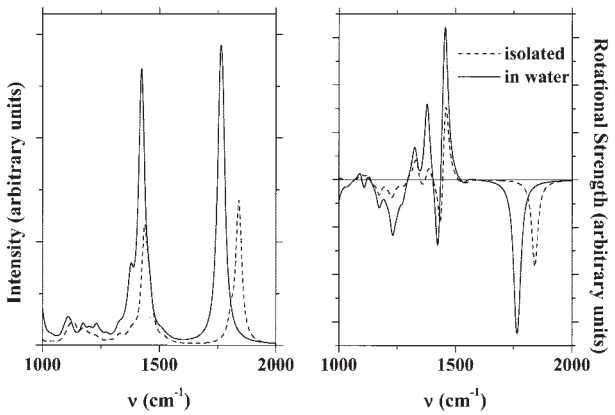

FIGURE 6. The simulated Boltzmann averaged IR (left) and VCD (right) spectra of neutral non-zwitterionic proline in the gas phase (dashed curve) and in aqueous environment (pure IEF, solid curve) in the 1000–2000 cm^{-1} frequency range.

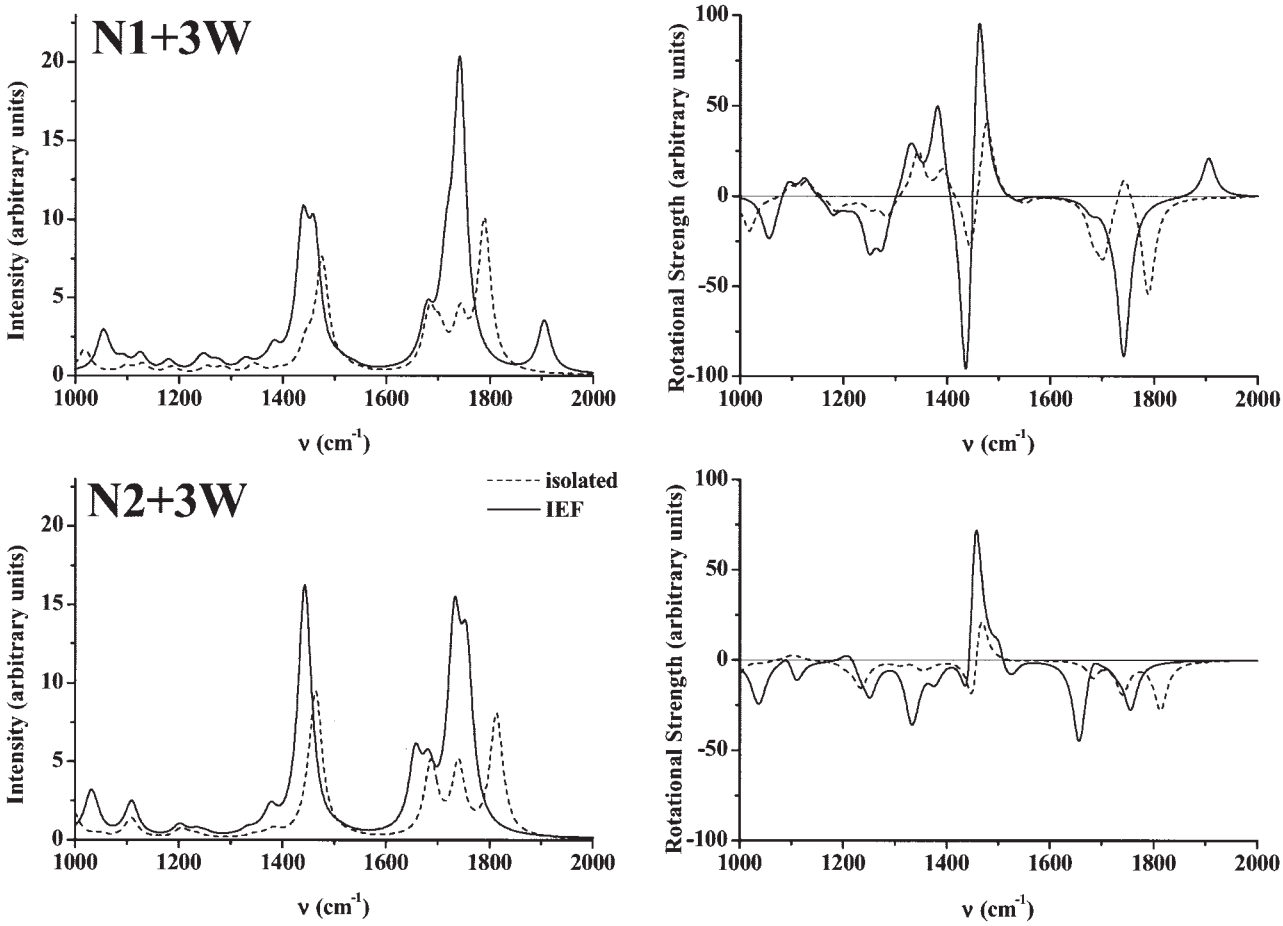

FIGURE 7. The simulated IR (left) and VCD (right) spectra in the 1000–2000 cm^{-1} frequency range for the individual neutral non-zwitterionic proline clusters **N1 + 3W** (top) and **N2 + 3W** (bottom). The dashed curves refer to the simulation for the isolated system, whereas the solid curves are obtained in aqueous environment.

changes in the relative intensity of the bands and in the overall appearance of the spectrum. Note in particular that the doubling of the carbonyl band, which is seen in the predicted spectrum for the isolated molecule (see the previous section), disappears completely in the presence of the environment, as a result of the very low population associated to the noninternally bonded conformations.

For the VCD spectrum, similar to IR, the inclusion of the IEF continuum affects the relative intensities of bands, whereas their sign does not change.

We have just discussed the effect of the introduction of continuum dielectric effects on proline vibrational spectra. An alternative strategy is to consider the effect of the solvent as due only to solute–solvent hydrogen-bond interactions. This is accomplished here through the evaluation of IR and VCD spectra with the **N + 3W** structures introduced and discussed in Section 3.1.1. Notice that all the potential specific sites of the carboxyl group to solvent are saturated in the **N + 3W** clusters.

The IR and VCD spectra of the **N + 3W** clusters are reported in Figure 7. To further refine the model, a continuum dielectric medium around the **N + 3W** clusters was included in some calculations.

The comparison of the **N + 3W** clusters spectra in Figure 7 with the corresponding of spectra of isolated proline in Figure 4 shows that, in the region between 1600 and 1800 cm^{-1}, the carbonyl stretching band superimposes to the water bending vibrations, thus resulting in an increase in the complexity of the spectrum. However, the presence of water molecules also causes a shift to lower frequencies of the characteristic bands of proline. In fact, the carbonyl stretching vibration, which in the case of **N1** in the gas phase is at 1840 cm^{-1}, moves to 1789 cm^{-1} in the **N1 + 3W** cluster. Further inclusion of the IEF continuum shifts the value to 1759 cm^{-1}

(**N1**) and to 1742 cm^{-1} (**N1 + 3W**). Note that the band at around 1900 cm^{-1} is a result of cluster water molecule bending vibrations.

As far as **N2** is concerned, the value in the gas phase (1841 cm^{-1}) lowers to 1813 cm^{-1} as a result of the inclusion of the three water molecules. The IEF continuum further shifts the value to 1771 cm^{-1} (**N2**) and to 1756 cm^{-1} (**N2 + 3W**), respectively.

In the 1400–1500 cm^{-1} region, involving the (carbonyl) C—O—H bendings, two bands are observed in the case of **N1** (independent of the further inclusion of the IEF continuum). These coalesce for **N2,** giving rise to different patterns in the two spectra.

The features of the IR spectra reflect into the VCD spectra. In this case, however, the inclusion of the IEF continuum in the **N1 + 3W** cluster yields a completely different pattern in the 1750–1850 cm^{-1} region.

The effect of the addition of a fourth explicit water molecule, this time H-bonded to the amino hydrogen, was estimated by performing calculations on conformers **N1** and **N2** surrounded by four water molecules. The resulting spectra are similar to those shown in Figure 7. The peak around 1460–1480 cm^{-1} shifts to higher frequencies by approximately 20–30 cm^{-1}, without changing its intensity. The shift is even lower for the peak above 1800 cm^{-1}. Thus the results of our analysis do not change significantly when adding a fourth explicit water molecule.

As already done in the previous sections, in Figure 8 Boltzmann-averaged spectra of proline calculated by exploiting the three solvation models—pure IEF, **N + 3W,** **N + 3W** (IEF)—are shown. The inclusion of the IEF continuum in the **N + 3W** model causes a large change in both frequencies and intensities. In particular, the number of visible bands varies. Generally the **N + 3W** (IEF) model is in better agreement with pure IEF than with the **N + 3W** model (which, we recall, accounts only for specific interactions). As already pointed out in the case of the neutral non-zwitterionic form, the sign of the bands in the VCD spectra is the same for all models. However, the number of the visible bands and their relative intensities change remarkably.

3.2.3. Effect of Protonation

To close the discussion of effects of the aqueous environment on the IR and VCD spectra of proline, we briefly discuss the effects of different protonation mechanisms. Averaged IR and VCD spectra for the cationic, anionic, and zwitterionic form of proline in water (pure IEF continuum approach) are

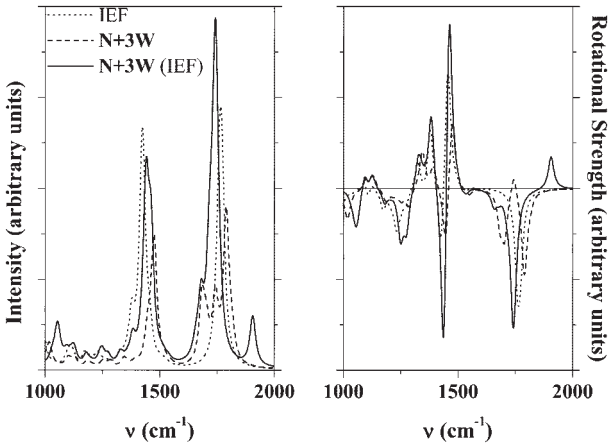

FIGURE 8. The simulated Boltzmann averaged IR (left) and VCD (right) spectra in the 1000–2000 cm^{-1} frequency range for the neutral non-zwitterionic proline in water obtained by using the three different solvation models (see text for details).

reported in Figure 9. The Boltzmann population of each conformer is given in Table III.

The protonation state of proline affects remarkably the overall appearance of the spectra. In fact, both the number and position of the bands change, as well as the intensity pattern. For the VCD spectra, the sign of the bands is also affected.

The cationic form of proline shows a carbonyl stretching peak at 1772 cm^{-1}, a NH_2 bending band at 1657 cm^{-1}, and a COH bending at 1174 cm^{-1}. In the case of the anion, the C═O stretching is at 1564 cm^{-1}, the NH bending at 1454 cm^{-1}, and a OCO bending band appears at 1403 cm^{-1}. Thus, as expected, the protonation state heavily influences the spectroscopic properties of the molecule. It is thus to be expected that the experimental spectra of proline might be very sensitive to the effective environment, and they are the result of a combination of the spectra of the various forms.

In modelling the effects of the aqueous environment on proline spectra it is, on the other hand, even more important to ascertain the differences arising when the zwitterionic forms are taken into account. It is well known that an equilibrium between the neutral non-zwitterionic and the zwitterionic forms exists in aqueous solutions of amino acids. In particular, the free energy values (see Table III) show that zwitterionic conformers are always more stable than neutral non-zwitterionic ones in solution.

Averaged IR and VCD spectra of zwitterionic proline are displayed in Figure 10.

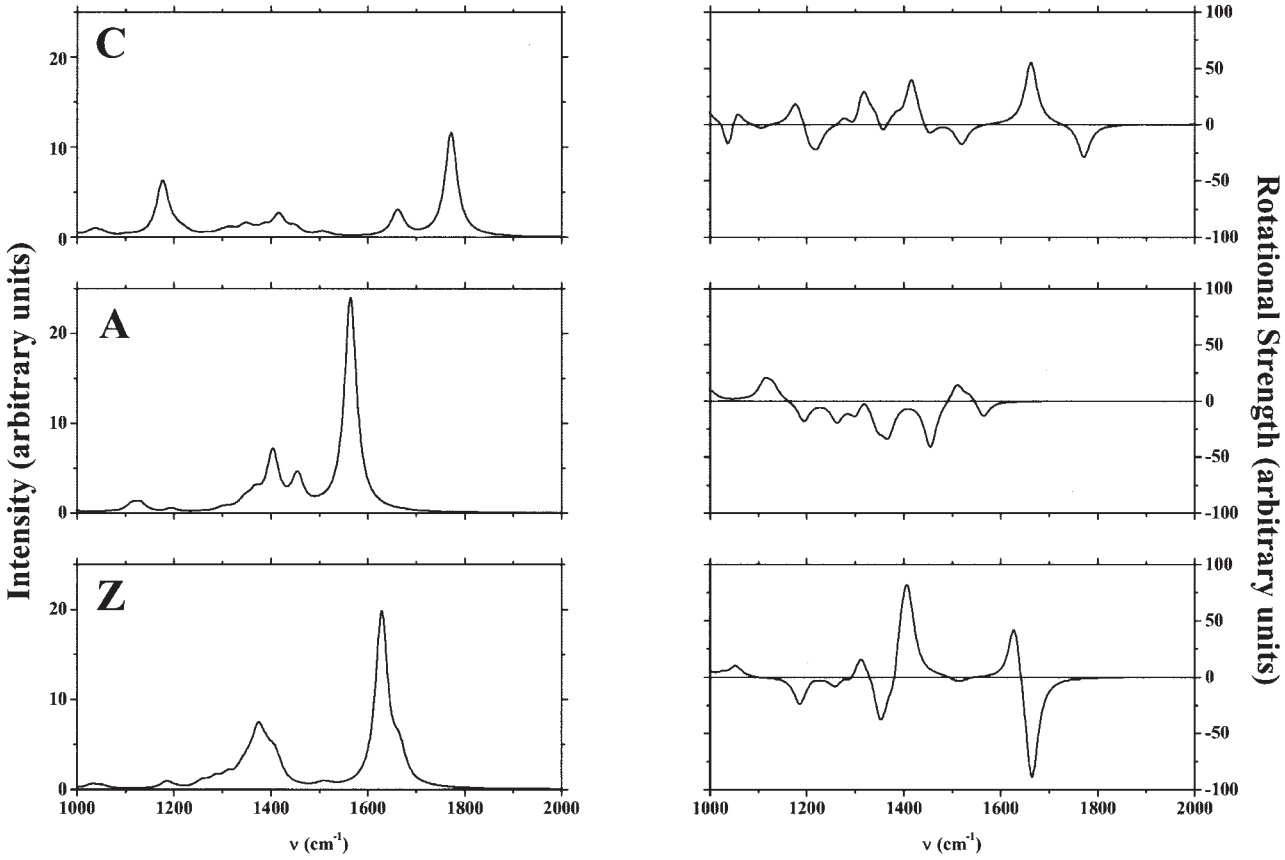

FIGURE 9. The simulated Boltzmann averaged IR (left) and VCD (right) spectra in the 1000–2000 cm^{-1} frequency range for the cationic (top), anionic (middle), and zwitterionic (bottom) forms of proline in water (pure IEF continuum model).

The carbonyl stretching band is nested with the NH_2 bending, thus giving rise to a complex structure in the 1630–1660 cm^{-1} range. The OCO bending vibration (coupled to the NH_2 bending) occurs at around 1400 cm^{-1}. In Figure 10, a comparison between the averaged spectra of the neutral non-zwitterionic and zwitterionic forms in the IEF continuum is also reported.

As was done for the neutral non-zwitterionic form of proline, the model has been refined to account for specific hydrogen bond effects. The calculated free energies of the $Z + 3W$ (IEF) conformers (see Fig. 2 and Table III) show that also in the case of H-bonded complexes the zwitterionic form is preferred in solution with respect to the neutral non-zwitterionic.

A comparison between averaged spectra IR and VCD spectra obtained in the **N + 3W** neutral non-zwitterionic and **Z + 3W** zwitterionic models in the IEF continuum is reported in Figure 11. Quite different frequency and intensity patterns are ob-

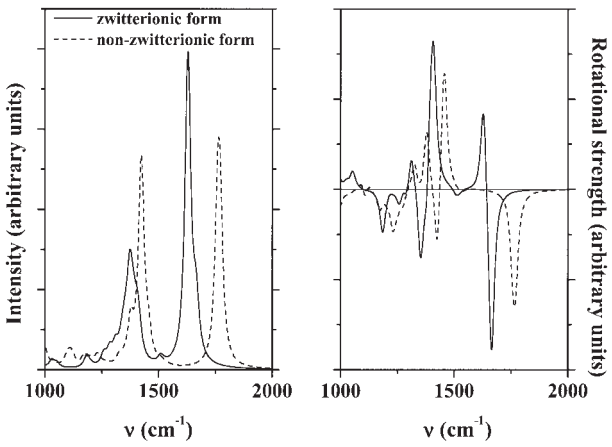

FIGURE 10. The simulated Boltzmann averaged IR (left) and VCD (right) spectra in the 1000–2000 cm^{-1} frequency range for the zwitterionic form of proline in water (pure IEF) compared to the non-zwitterionic form (pure IEF).

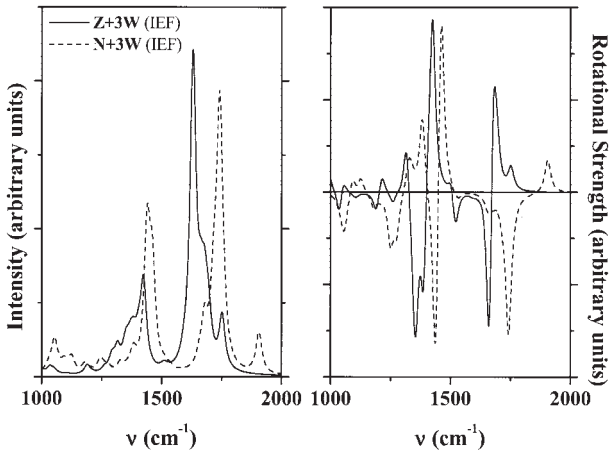

FIGURE 11. The simulated Boltzmann averaged IR (left) and VCD (right) spectra in the 1000–2000 cm^{-1} frequency range of neutral non-zwitterionic and zwitterionic proline in water obtained for the cluster structures in the IEF continuum (see text).

served. In particular, as a result of the deprotonation the C═O bands are shifted to lower frequency values. The bending vibrations around 1450 cm^{-1} are shifted to lower frequencies and they give rise to a complex and broad band. Note also that the water bending band is shifted. An analogous analysis of the VCD spectra shows completely different behavior for the neutral non-zwitterionic and zwitterionic forms. Not only frequencies and relative intensities change remarkably but also the sign of the band are inverted in some instances.

4. Summary and Conclusions

We have carried out a detailed ab initio conformational analysis of proline both as isolated molecule and in water solution with the aim of analyzing solvent effects on IR and VCD spectra. The quantum mechanical approach, based on DFT with the choice of B3LYP functional and employed for geometry optimizations and the simulation of the spectra, relies on the polarizable dielectric continuum model (PCM) in its integral equation formalism (IEF). Neutral (including zwitterionic), protonated and deprotonated structures were analyzed. The effect of specific (hydrogen bond) solute–solvent interactions arising due to the unique features of the aqueous environment, and which can only partially be estimated by a pure continuum approach, was accounted for by introducing cluster structures including explicitly three water molecules arranged around the proline moiety.

The conformational analysis, yielding information on free energy and Boltzmann populations for each individual conformer, gives insights on the distribution among different conformers of proline in the gas phase and in water. Although the effect of environment on the geometry of a given conformer is relatively small, the ordering as determined by the Boltzmann population may change dramatically, and, with the stabilization provided by the solvent to H-bonded and charged dipolar structures, it leads in some cases to the disappearance in the aqueous environment of some of the low-lying gas-phase-favored conformational structures.

The effect of the environment on IR and VCD spectra, analyzed here in the 1000–2000 cm^{-1} frequency range, is remarkable, causing shifts to lower frequencies and changes in intensities and, in the case of VCD, also changes of band sign. The structural model employed (proline moiety, or proline with three water molecules in the cluster, with or without inclusion of the IEF continuum) influences remarkably the outcome in some cases. Also, protonation has a noticeable effect on the predicted spectra, as does the balance of zwitterionic and non-zwitterionic neutral structures in solution.

References

1. MacArthur, M.; Thornton, J. M. J Mol Biol 1991, 218, 397.
2. Richardson, J. S.; Richardson, D. C. Science 1998, 240, 1648.
3. Milner-White, E. J.; Bell, L. H.; Maccallum, P. H. J Mol Biol 1992, 228, 725.
4. Richardson, J. S. In Advances in Protein Chemistry, Vol. 34; Anfinsen, C. B.; Edsall, J. T.; Richards, F. M., Eds., Academic Press: New York, 1981.
5. Nemethy, G.; Printz, M. P. Macromolecules 1972, 6, 755.
6. Piela, L.; Nemethy, G.; Sheraga, H. A. Biopolymers 1987, 26, 1587.
7. Chou, P. Y.; Fasman, G. D. Biochemistry 1974, 13, 211.
8. Sankararamakrishnan, R.; Vishveshwara, S. Biopolymers 1990, 30, 287.
9. Dasgupta, S.; Bell, J. A. J Peptide Protein Res 1993, 41, 499.
10. Hagerman, A. E.; Butler, L. G. J Biol Chem 1981, 256, 4494.
11. Baxter, N. J.; Lilley, T. H.; Haslam, E.; Williamson, M. P. Biochemistry 1997, 36, 5566.
12. Bronco, S.; Cappelli, C.; Monti, S. J Phys Chem B 2004, 108, 10101.
13. Kayushina, R. L.; Vainstein, B. K. Sov Phys Crystallogr 1966, 10, 698.
14. Balasubramanian, R.; Lakshminarayanan, A. V.; Sabesan, M. N.; Tegoni, G.; Venkatesan, K.; Ramachandran, G. N. Int J Pept Protein Res 1971, 3, 25.

15. DeTar, D. F.; Luthra, N. P. J Am Chem Soc 1977, 99, 1232.
16. Iijima, K.; Tanaka, K.; Onuma, S. J Mol Struct 1991, 246, 257.
17. Iijima, K.; Beagley, B. J Mol Struct 1991, 248, 133.
18. Brown, R. D.; Godfrey, P. D.; Storey, J. W. V.; Bassez, M. P. J Chem Soc Chem Commun 1978, 547.
19. Suenram, R. D.; Lovas, F. J. J Mol Spectrosc 1978, 72, 372.
20. Suenram, R. D.; Lovas, F. J. J Am Chem Soc 1980, 102, 7180.
21. Schaefer, L.; Sellers, H. L.; Lowas, F. J.; Suernam, R. D. J Am Chem Soc 1980, 102, 6566.
22. Godfrey, P. D.; Brown, R. D. J Am Chem Soc 1995, 117, 2019.
23. Lovas, F. J.; Kawashima, Y.; Grabow, J. U.; Suenram, R. D.; Freser, G. T.; Hirota, E. Astrophys J 1995, 455, 201.
24. McGlone, S. J.; Elmes, P. S.; Brown, R. D.; Godfrey, P. D. J Mol Struct 1999, 486, 255.
25. Godfrey, P. D.; Firth, S.; Haterley, L. D.; Brown, R. D.; Pierlot, A. P. J Am Chem Soc 1993, 115, 9687.
26. Haasnoot, C. A. G.; DeLeeuw, F. A. A. M.; DeLeeuw, H. P. M.; Altona, C. Biopolymers 1981, 20, 1211.
27. Debies, T. P.; Rabalais, J. W. J Electron Spectrosc Relat Phenom 1974, 3, 315.
28. Klasinc, L. J. J Electron Spectrosc Relat Phenom 1976, 8, 161.
29. Reva, I. D.; Stepanian, S. G.; Plokhotnichenko, A. M.; Radchenko, E. D.; Sheina, G. G.; Blagoi, Y. P. J Mol Struct 1994, 318, 1.
30. Herlinger, A. W.; Long, T. W. II. J Am Chem Soc 1970, 92, 6481.
31. Stepanian, S. G.; Reva, I. D.; Radchenko, E. D.; Adamowicz, L. J Phys Chem 2001, 105, 10664.
32. Sapse, A. M.; Mallah-Levy, L.; Daniels, S. B.; Ericson, J. J Am Chem Soc 1987, 109, 3526.
33. Tarakeshwar, P.; Manogaran, S. J Mol Struct (Theochem) 1996, 365, 167.
34. Ramek, M.; Kelterer, A. M.; Nikolic, S. Int J Quantum Chem 1997, 65, 1033.
35. Császár, A. G.; Perczel, A. Prog Biophys Mol Biol 1999, 71, 243.
36. Czinki, E.; Császár, A. G. Chem Eur J 2003, 9, 2008.
37. Benzi, C.; Improta, R.; Scalmani, G.; Barone, V. J Comp Chem 2002, 23, 341.
38. Pecul, M.; Ruud, K.; Rizzo, A.; Helgaker, T. J Phys Chem A 2004, 108, 4269.
39. Coriani, S.; Pecul, M.; Rizzo, A.; Jørgensen, P.; Jaszuński, M. J Chem Phys 2002, 117, 6417.
40. Becke, A. D. J Chem Phys 1993, 98, 5648.
41. Becke, A. D. Phys Rev A 1988, 38, 3098.
42. Lee, C.; Yang, W.; Parr, R. G. Phys Rev B 1988, 37, 785.
43. Stephens, P. J.; Devlin, F. J. Chirality 2000, 12, 172.
44. Cancès, E.; Mennucci, B. J Math Chem 1998, 23, 30.
45. Cancès, E.; Mennucci, B.; Tomasi, J. J Chem Phys 1997, 107, 3032.
46. Mennucci, B.; Cancès, E. J Phys Chem B 1997, 101, 10506.
47. Miertus, S.; Scrocco, E.; Tomasi, J. Chem Phys 1981, 55, 117.
48. Cammi, R.; Tomasi, J. J Comp Chem 1995, 16, 1449.
49. Tomasi, J.; Persico, M. Chem Rev 1994, 94, 2027.
50. Cramer, C. J.; Truhlar, D. G. Chem Rev 1999, 99, 2161.
51. Cammi, R.; Cappelli, C.; Corni, S.; Tomasi, J. J Phys Chem A 2000, 104, 9874.
52. Cappelli, C.; Corni, S.; Mennucci, B.; Cammi, R.; Tomasi, J. J Phys Chem A 2002, 106, 12331.
53. Scott, A. P.; Radom, L. J Phys Chem 1996, 100, 16502.
54. Halls, M. D.; Schlegel, H. B. J Chem Phys 1998, 109, 10587.
55. Frisch, M. J.; Trucks, G. W.; Schlegel, H. B.; Scuseria, G. E.; Robb, M. A.; Cheeseman, J. R.; Montgomery, J. A., Jr.; Vreven, T.; Kudin, K. N.; Burant, J. C.; Millam, J. M.; Iyengar, S. S.; Tomasi, J.; Barone, V.; Mennucci, B.; Cossi, M.; Scalmani, G.; Rega, N.; Petersson, G. A.; Nakatsuji, H.; Hada, M.; Ehara, M.; Toyota, K.; Fukuda, R.; Hasegawa, J.; Ishida, M.; Nakajima, T.; Honda, Y.; Kitao, O.; Nakai, H.; Klene, M.; Li, X.; Knox, J. E.; Hratchian, H. P.; Cross, J. B.; Adamo, C.; Jaramillo, J.; Gomperts, R.; Stratmann, R. E.; Yazyev, O.; Austin, A. J.; Cammi, R.; Pomelli, C.; Ochterski, J. W.; Ayala, P. Y.; Morokuma, K.; Voth, G. A.; Salvador, P.; Dannenberg, J. J.; Zakrzewski, V. G.; Dapprich, S.; Daniels, A. D.; Strain, M. C.; Farkas, O.; Malick, D. K.; Rabuck, A. D.; Raghavachari, K.; Foresman, J. B.; Ortiz, J. V.; Cui, Q.; Baboul, A. G.; Clifford, S.; Cioslowski, J.; Stefanov, B. B.; Liu, G.; Liashenko, A.; Piskorz, P.; Komaromi, I.; Martin, R. L.; Fox, D. J.; Keith, T.; Al-Laham, M. A.; Peng, C. Y.; Nanayakkara, A.; Challacombe, M.; Gill, P. M. W.; Johnson, B.; Chen, W.; Wong, M. W.; Gonzalez, C.; Pople, J. A. Gaussian 03, Revision A.1; Gaussian, Inc.: Pittsburgh, PA, 2003.
56. Cappelli, C.; Corni, S.; Cammi, R.; Mennucci, B.; Tomasi, J. J Chem Phys 2000, 113, 11270.
57. London, F.; J Phys Radium (Paris) 1937, 8, 397.
58. Ditchfield, R. D. J Chem Phys 1972, 56, 5688.
59. Ditchfield, R. D. Mol Phys 1974, 27, 789.
60. Cammi, R.; Mennucci, B.; Tomasi, J. J Chem Phys 1999, 110, 9627.